On the origin of the ring system of (10199) Chariklo

M. D. Melita[1], Duffard, R.[2], Ortiz J.L.[2]

melita@iafe.uba.ar

[1] IAFE (UBA-CONICET) y FCAG (UNLP).
[2] Instituto de Astrofísica de Andalucía (CSIC). Granada. España.

Layout

Astrophysical Background:

- (10199) Chariklo
- The Centaurs
- (10199) Chariklo Ring System

Formation scenarios:

- Classical Roche limit & Tidal evolution
- Material ejected by a collision on the body of the asteoriod
- Breakup of a satellite of (10199) Chariklo due to a catastrophic collision
- Cometary-like activity (Pan & Wu 2016, arXiv:1602.01769)

- Discussion

Centaur asteroids

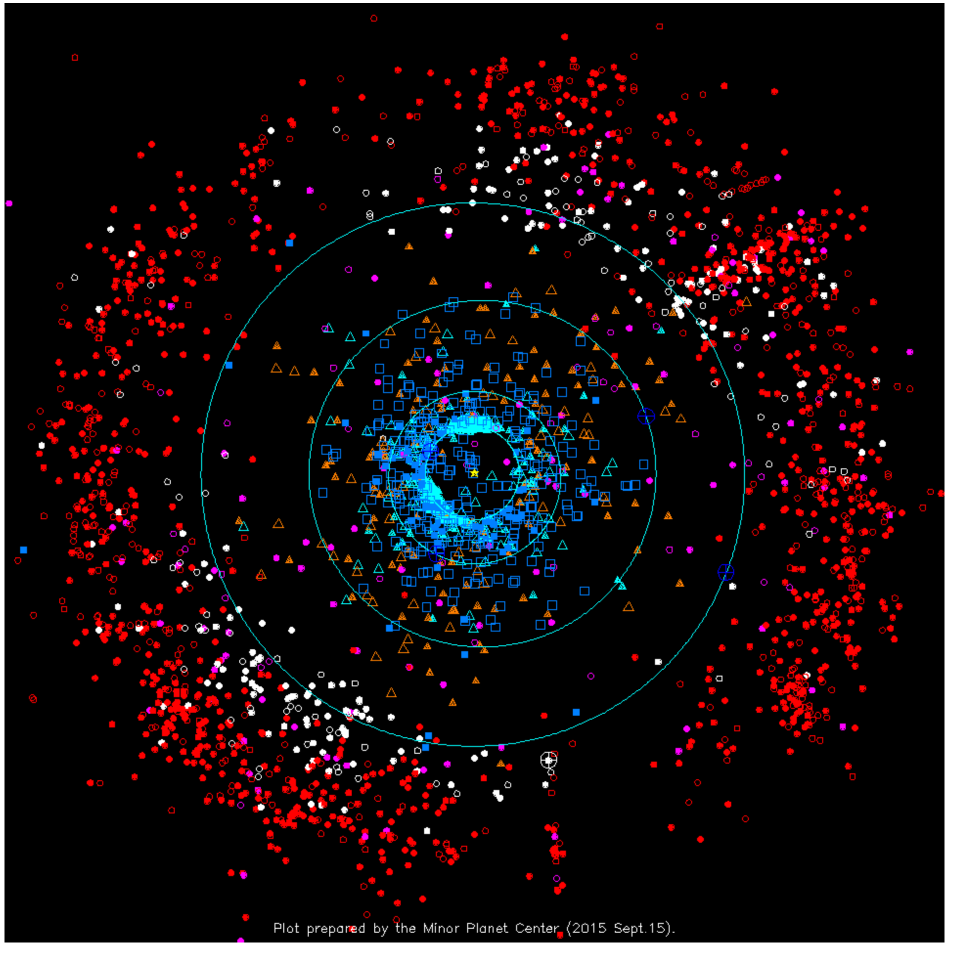

The Centaurs
Features and Peculiarities

- It is a transitinal population (Levison & Duncan 1997) with dynamical lifetimes between the planets of $\sim 10^4 - 10^5$ yr.
- The observed surface properties are not a simple juxtaposition of the properties of the bodies at the origin (TNOs) or as end-states (JFCs), i.e. The color distribution is bimodal (Tegler & Romanishin 2003, Melita & Licandro 2012), as observed in small TNOs (Peixinho 2014).
- Cometary-like comas have been observed on some members. e.g. (2060) Chiron, sometimes attributed to phase changes of water-ice (Jewitt 2009).
- Only class of asteroids where rings have been detected.

(10199) Chariklo

- H = 6.6
- m$_V$ = 18.5
- p = 4.5 %
- a = 15.75 AU
- e = 0.15
- i = 23 deg
- R$_1$ = R$_2$ = 122 km
- R$_3$ = 117 km
- M($\rho = 1 g/cm^3$) = 7 10^{18} kg
- Colors: | B-V | = 0.86 (Grey)

Discovery of the ring system

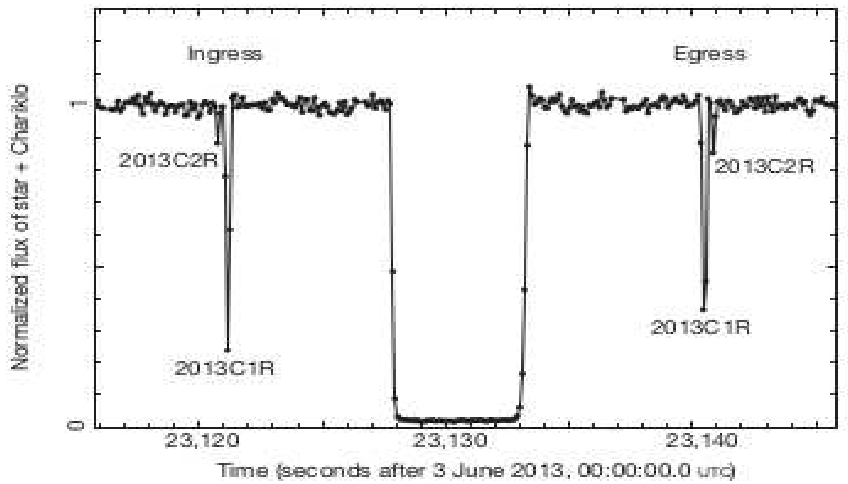

Figure 1 | Light curve of the occultation by the Chariklo system. The data were taken with the Danish 1.54-m telescope (La Silla) on 3 June 2013, at a rate of almost 10 Hz and with a long-pass filter and a cut-off below 650 nm, limited at long wavelengths by the sensitivity of the charge-coupled-device chip (Supplementary Information). Aperture photometry provided the flux from the target star and a fainter nearby reference star. Low-frequency sky transparency variations were removed by dividing the target flux by an optimal running average of 87 data points (8.7 s) of the reference star, resulting in a final signal-to-noise ratio of 64 per data point. The sum of the stellar and Chariklo fluxes has been normalized to unity outside the occultation. The central drop is caused by Chariklo, and two secondary events, 2013C1R and 2013C2R, are observed, one at ingress (before the main Chariklo occultation) and then at egress (after the main occultation). A more detailed view of these ring events is shown in Fig. 3.

Occultation Band

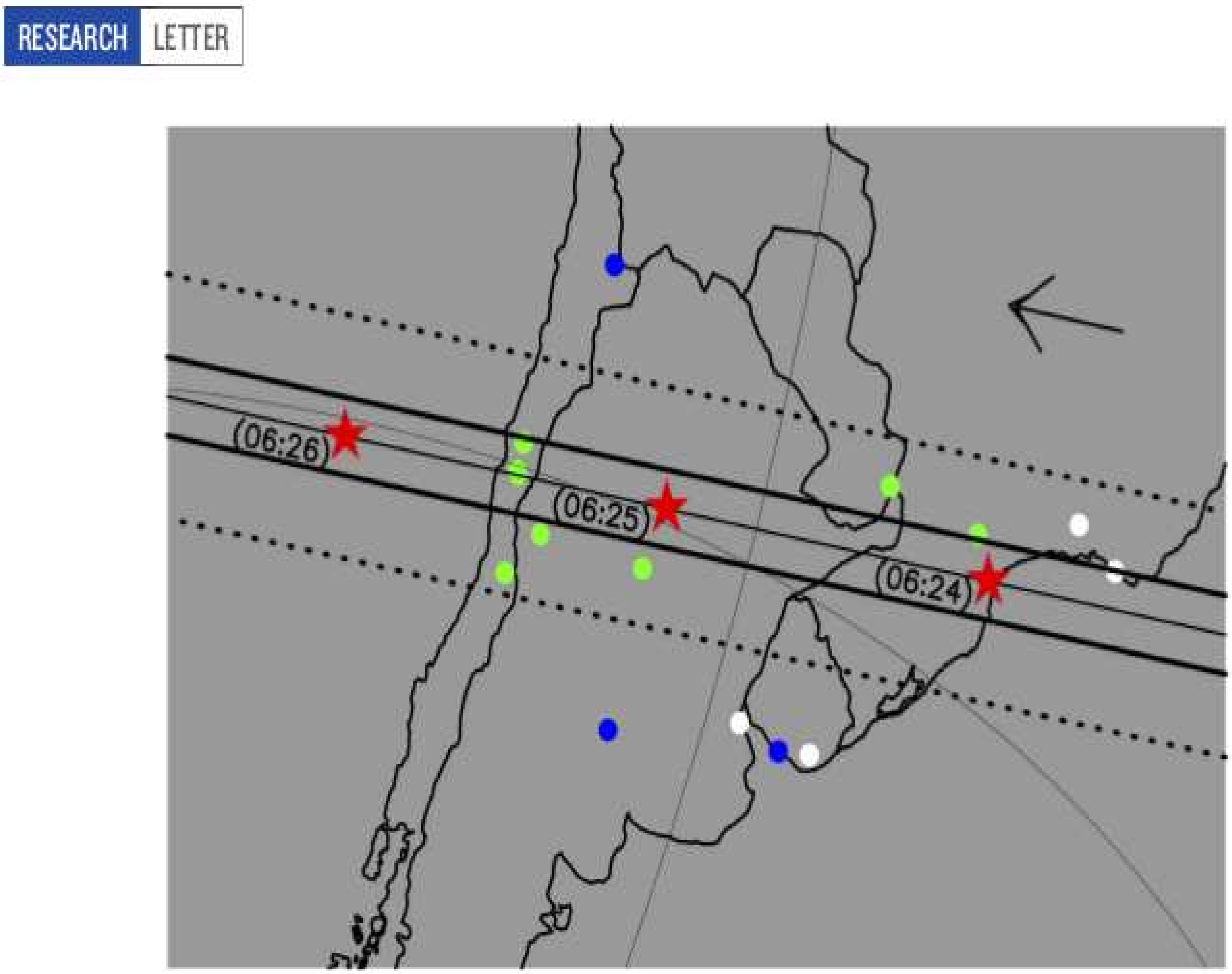

Extended Data Figure 1 | The Chariklo 3 June 2013 occultation campaign. The continuous straight lines indicate Chariklo's shadow track on Earth, and the dotted lines correspond to the ring shadow, as reconstructed from our post-occultation analysis. The shadows move from right to left, as indicated. The red stars indicate the centre of Chariklo's shadow at various times (UTC). The green dots are the sites where the occultation was detected. The blue dots are the sites that had obtained data but did not detect the event, and the white ones are the sites that were clouded out (Extended Data Table 1).

Modelled geometry of the system

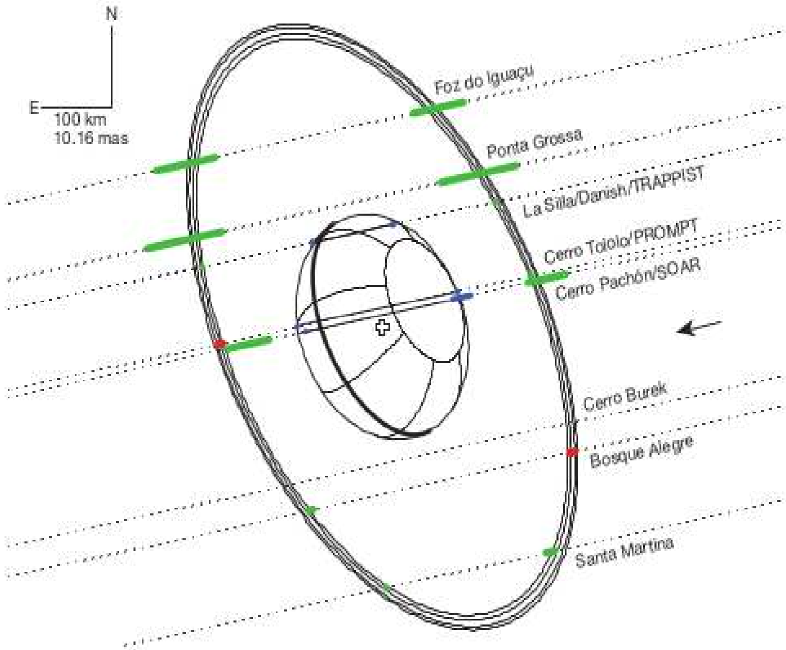

Figure 2 | Chariklo ring system. The dotted lines are the trajectories of the star relative to Chariklo in the plane of the sky, as observed from eight sites (Supplementary Information), the arrow indicating the direction of motion. The green segments represent the locations of ring C1R observed at each station (1σ uncertainty). For clarity, we have not plotted the detections made at the TRAPPIST and 0.275-m telescopes (at La Silla and Bosque Alegre, respectively) because they have larger error bars than their local counterparts, and would supersede the corresponding green segments. Two ring events occurred during camera readout times (red segments) at Bosque Alegre and Cerro Tololo, and also provide constraints on the ring orbit. The ring events are only marginally detected at Cerro Burek, but the signal-to-noise ratio is not sufficient to put further constraints on the ring orbit and equivalent width. An elliptical fit to the green and red segments (excluding, because of timing problems (Supplementary Information), the SOAR events at Cerro Pachón) provides the centre of the rings (open cross), as well as their sizes, opening angle and orientation (Table 1). Chariklo's limb has been fitted to the two chords' extremities (blue segments) obtained at La Silla and Cerro Tololo, assuming that the centres of Chariklo and the rings, as well as their position angles, coincide. This is expected if Chariklo is a spheroid, with a circular ring orbiting in the equatorial plane (see text and Supplementary Information).

The "Gap"

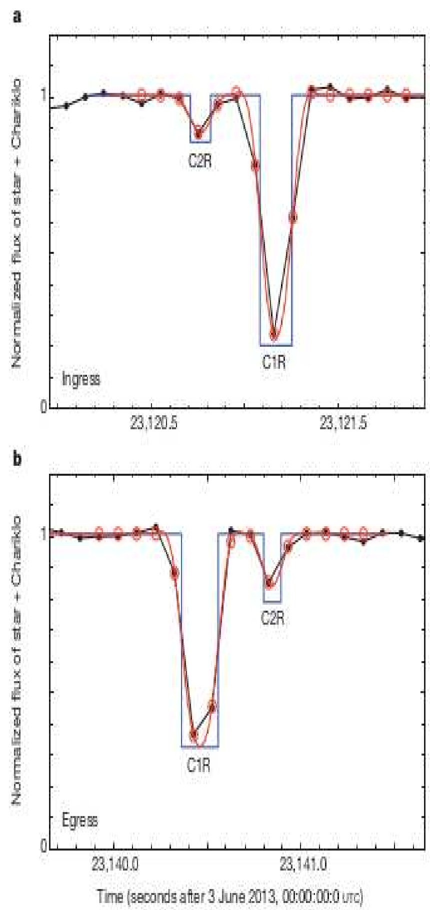

tary activity has been detected around Chariklo).

About 5% of the Centaur and trans-Neptunian population[23] are known to have satellites. Although the large satellites are thought to result from three-body captures, their small counterparts are more likely to form from impacts[24], or rotational disruptions[25], and possibly re-accretion from a disk remaining after that event. So far, no observations have shown satellites around Chariklo (the rings span at most 0.04'' around the primary object, making direct detections of associated small satellites a challenge). Several origins for Chariklo's rings can be proposed, all relying on a debris disk in which the largest fragments acted as shepherds for the smaller material. The first possibility is that an impactor excavated icy material from Chariklo's outer layers, destroyed a pre-existing satellite or was itself disrupted during the impact. The second is that a debris disk formed from a rotational disruption of the main body or was fed by cometary-like activity. Third, two pre-existing satellites

Figure 3 | Fits to the Danish ring events. a, b, The red curves are synthetic occultation profiles produced by semi-transparent bands with square-well profiles (the blue lines), after convolution by Fresnel diffraction, observed bandwidth, the stellar radius projected at Chariklo, and the finite integration time. The open red circles are the values of the model for the times corresponding to the observed data points (black points) at the ingress (**a**) and egress (**b**). The χ^2 values per degree of freedom of the fits to the four ring events vary from 0.4 to 1.2 (Extended Data Table 2). This indicates satisfactory fits, and shows that the events are compatible with sharp-edged rings. The resulting widths and optical depths of rings C1R and C2R are listed in Table 1, after the appropriate projections into the plane of the rings have been performed. Extended Data Table 3 shows that the widths and optical depths of C1R at the Danish 1.54-m telescope differ moderately but significantly between ingress and egress. The equivalent depth of C1R changes by 21% between ingress and egress. Similar variations are observed in Uranus's narrow rings, and might be associated with normal mode oscillations that azimuthally modulate the width and optical depth of the rings[10]. Differences between C2R ingress and egress are marginally significant.

Features of the ring system

Braga-Rivas et al. (2014). Nature. 72. 508.

- R$_{in}$ = 390.6 $\pm$ 3.3 km
- τ_{O_1} = 0.45
- R_{out} = 404.8 $\pm$ 3.3 km
- τ_{O_2} = 0.05
- W = 14.2 $\pm$ 0.2 km
- W_{Gap} = 8.7 $\pm$ 0.4 km
- τ_{Gap} ¡ 0.004
- Mass $\approx 10^{13}$ kg
- Orbital Period: $T \approx 0.82\ d$
- Frecuencies: $n \approx 8.83\ 10^{-5}\ s^{-1} = 7.6\ d^{-1}$
- To note: $n \approx n_{Urano} \approx n_{SaturnoExt}$
- $\tau \approx \tau_{Urano} \approx \tau_{SaturnoExt}$

Observed features point to the existence of Shepherd Satellites.
Confirmation of Chariklo's rings have been made at one further occultation event, revealing an eccentric figure (Bérard et al., DPS 11/2015).

- T$_{\nu} \approx 10^4$ años
- T$_{PR} \approx 10^6$ años
- $R_{Sat_Pastor} \approx$ 3 km ($\rho = 1 g/cm^3$)
- $R_{Sat_Gap} \approx$ 1 km ($\rho = 1 g/cm^3$)

The case of a ring about (2060) Chiron

Ortiz J.L. et al. (2015):

A&A proofs: manuscript no. 24461_ja-final

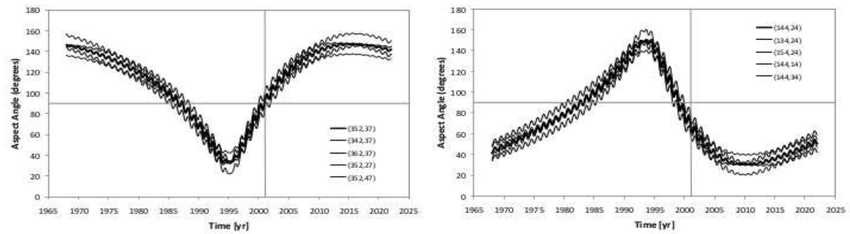

Fig. 4. Aspect angle versus time. Left panel: The continuous line shows the aspect angle of Chiron's rings as a function of time for the nominal pole direction that we obtained from the analysis of the occultations of the rings (λ= 352 ±10 °, β= 37 deg ± 10 °). The rest of the lines correspond to solutions within the uncertainties of the nominal pole. The vertical and horizontal lines are shown to highlight that in 2001 the aspect angle of the rings was 90 degrees. The right panel shows the aspect angle as a function of time for the other pole direction (λ=(144±10)°, β=(24±10)°).

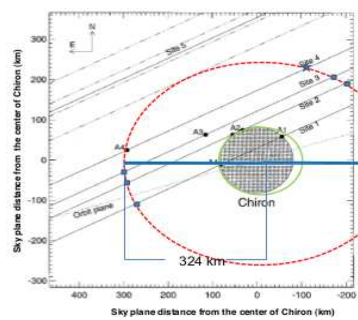

Fig. 3. Stellar occultation in 1993: Adapted from Fig. 5 of Bus et al. (1996) in which the sky plane for the region surrounding Chiron is shown. The ellipse (dashed line) shows the ring of Chiron that would cause the A4 feature and is compatible with the orientation derived from the two pole solutions derived from the 2011 occultation. The position angle is 1 degree, and the aspect angle is 30 degrees or 150 degrees. The star symbol indicates another intersection of the ring with the star path for site 4, where another secondary event should have been detected from site 4 (see text), and the small squares show locations where secondary events should have been detected if the observations at the particular observing sites obtained data with high signal-to-noise ratio, which was not the case. The disk of Chiron is shown based on a circular fit to the occultation chords, but in green we show an alternative disk of Chiron. See main text.

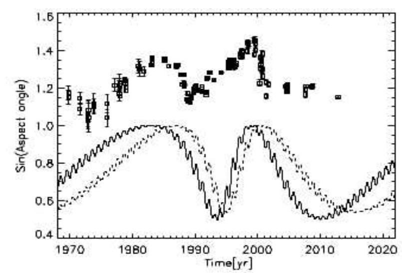

Fig. 5. Coincidence of the brightness minima with aspect angle near 90 degrees. With a continuous line we show the sine of the aspect angle of Chiron as a function of time using the preferred pole solution (λ=144°, β=24°). The dotted line corresponds to the other solution for the pole direction (λ=352°, β=37°). The square symbols represent the absolute magnitude of Chiron from Belskaya et al. (2010) divided by a factor 5 for easier viewing. As can be seen, there is coincidence between aspect angle and absolute magnitude, but there is a shift between the aspect angle maxima and the absolute magnitude maxima for the λ=352°, β=37° pole solution.

as a function of time. We do this to illustrate when the rings are edge-on (maxima of the curves) and to compare the maxima in the curves with the absolute magnitude measurements. As can be seen, the second pole solution (λ=(144±10)°, β=(24±10)°) gives a better match to the times when the maxima in absolute magnitude (brightness minima) are reached. Our explanation of this coincidence is that the rings have an important effect on the long-

Formation scenarios

- o Tidal disruption
- o Collisions: On the asteroid/ On a satellite
- X Cometary-like activity

Any scenario should be size dependent,
why we do not observe rings about larger asteroids?
and explain the existence of shepherds.

Roche´s Classical limit, d

Murray & Demott (1999)

$$\boxed{d = R_s \left(3 \frac{M}{m}\right)^{1/3}}$$

where:

Mass of (10199) Chariklo: $M = \frac{4\,\pi}{3}\,\rho A^2 C$
Principal axes of (10199) Chariklo: $A = B, C$
Density of (10199) Chariklo: ρ
Mass of the satellite : $m = \rho_s A_s^3 \epsilon$
Density of the satellite: ρ_s
Principal axes of the sattellite: $A_s = B_s, C_s$
Mean radius of the satellite: R_s

$\epsilon = \frac{4\,\pi}{3}\,\gamma$
$\gamma_s = \frac{C_s}{A_s}$
$\delta = \rho/\rho_s$

$$\boxed{d = R_s \left(3 \frac{\delta}{\gamma_s} \frac{A^2 C}{R_s^3}\right)^{1/3}}$$

The Classical Roche limit of (10199) Chariklo

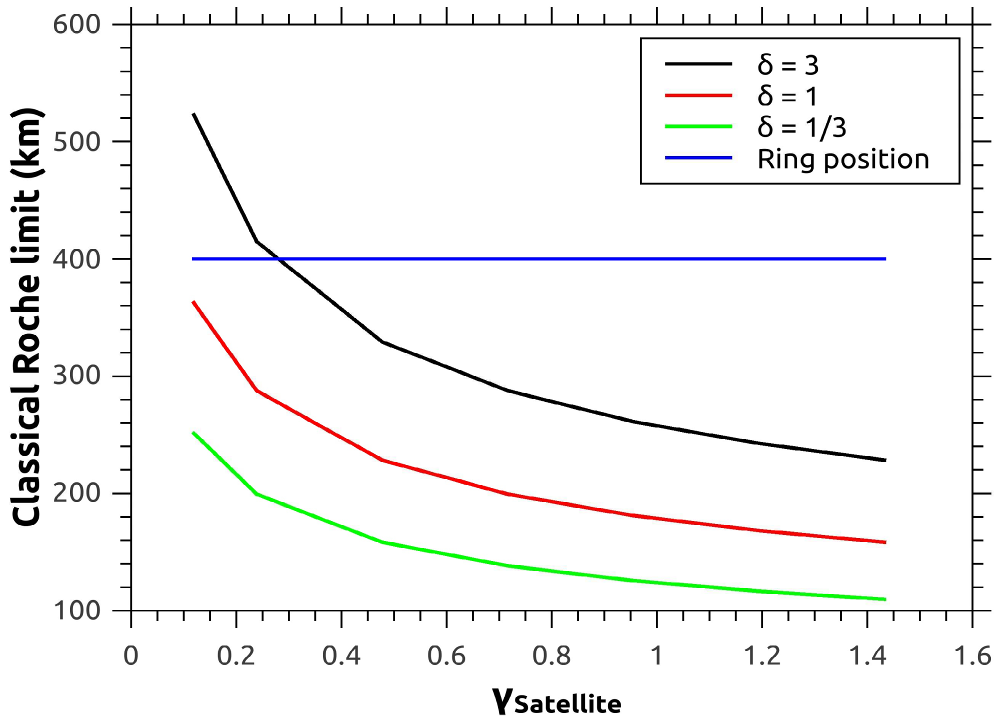

Breakup distance and Shepherd Satellites

Dobrovolskis (1990)

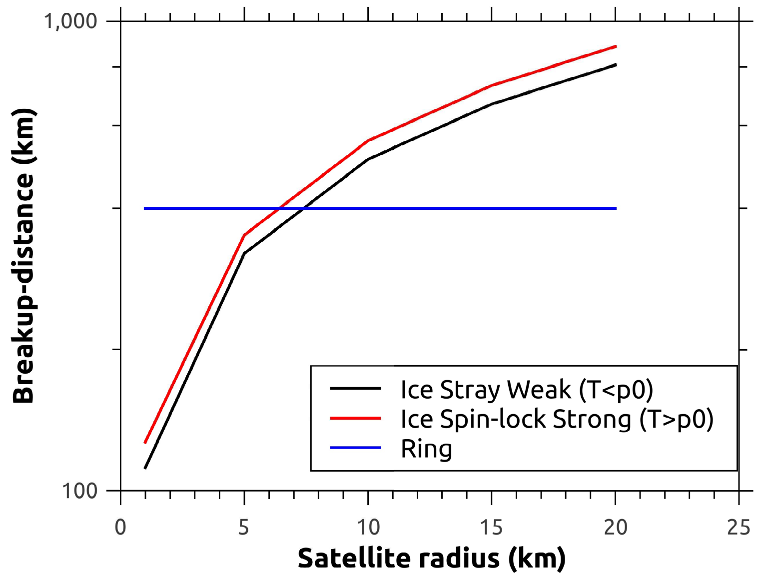

Tidal Evolution

We only retain from the tidal potential the most significant order in $\cos\psi$ and R_S/r, where ψ is the angle between the asteroid and the satellite.

Classical formulation of lag: l, i.e. $sin(l) = 1/Q$, where Q is te quality factor.

Asteroid rotation and the satétilie orbit in the same sense and outside co-rotation $(\Omega < n)$, thus (Murray and Dermott 1999):

$$\boxed{\dot{a} \approx -\frac{3k_2}{2\alpha Q}\, a\, n\, \frac{m}{M}\left(\frac{A}{a}\right)^5}$$

Where:
Semimajor axis: a
Rotación angular velocity: Ω
Orbital angular velocity: n
Love number : $k_2 = \frac{1.5}{(1+\bar{\mu})}$.
Effective rigidity: $\bar{\mu} = \frac{19\mu}{(2\rho g(A)A)}$
Gravity at the surface of the asteroid: $g(A)$
Mean Rigity of water ice: $\mu = 4Nm^{-2}$

Therefore, $k_2 = 1.6\;10^{-4}$, si $\rho = 1gcm^{-3}$.

Tidal travel-time

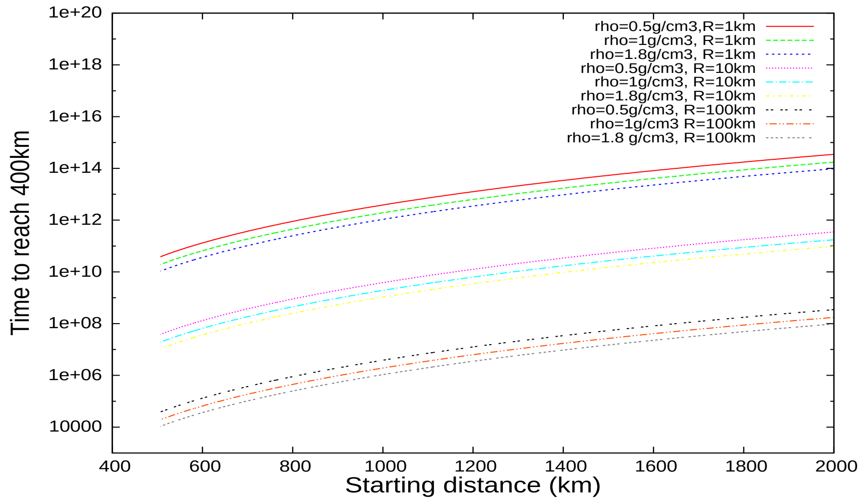

$$\boxed{\tau_{12} = \frac{2}{13}\, C_T\, \left(a_2^{13/2} - a_1^{13/2}\right)}$$

$$\boxed{C_T = \frac{2}{9}\, \left(\frac{Q}{k_2}\right)\, \left(\frac{M}{m}\right)\, \left(\sqrt{\frac{1}{A^5 G M}}\right).}$$

Frecuency distribution in the SS

Source: MPC

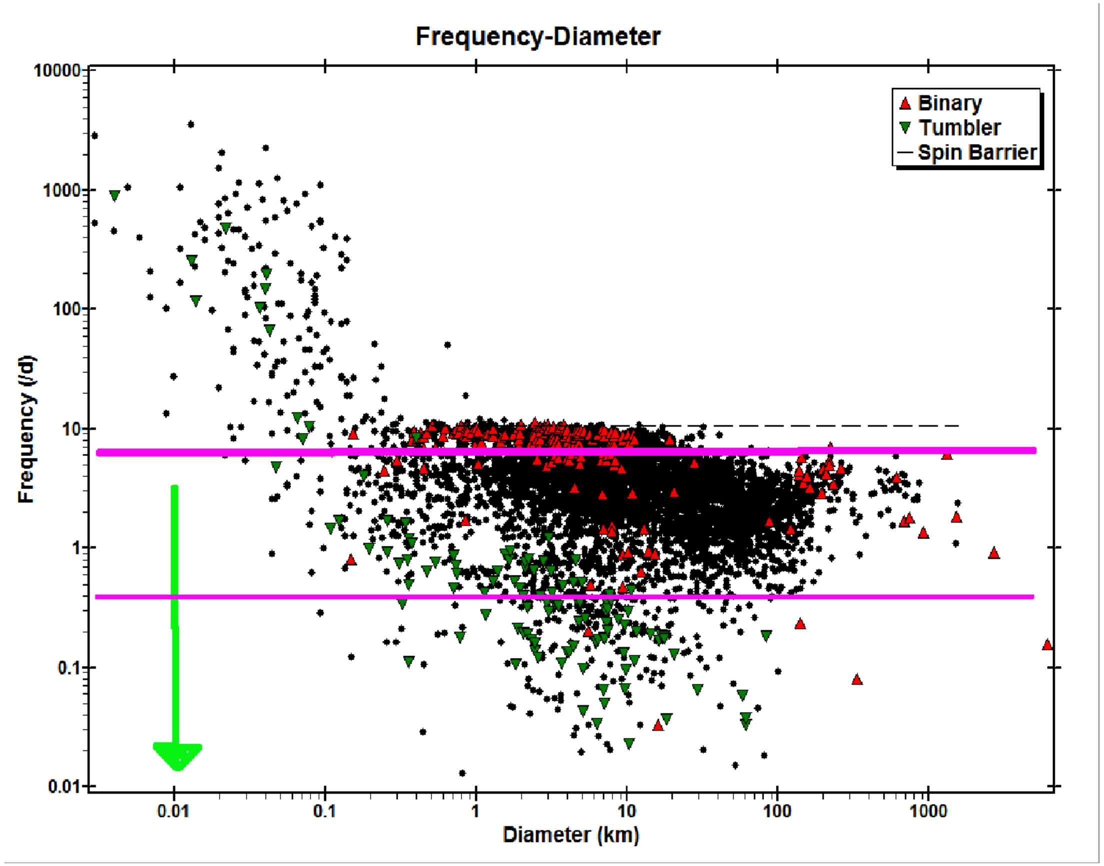

Collision on (10199) Chariklo

Housen & Holsapple (2011) - Gravity regime:

$$\boxed{m_e(v > v_e) = \frac{3k}{4\pi}\frac{\rho}{\rho_S}\left[\left(\frac{x}{c}\right)^3 - n_1^3\right]}$$

$$\boxed{v_e(x) = C_1\; v_r\; \left[\frac{x}{c}\left(\frac{\rho}{\rho_S}\right)^{\nu}\right]^{-1/\mu}\left(1 - \frac{x}{n_2 R}\right)^p}$$

x: distance to the center of the crater

$R = (R_1^2 R_3)^{1/3}$

Scaling constants for water ice:

$\nu = 0.4$

$k = 0.3$

$p = 0.3$

$n_1 = 1.2$

$n_2 = 1.3$

We search for:

$$\boxed{\frac{-GM}{2R_o} < \frac{-GM}{R} + \frac{1}{2}v_e(x) < \frac{-GM}{2R_i}}$$

$$\boxed{M_{RS} \sim M(v > v_i) - M(v > v_o)}$$

Results

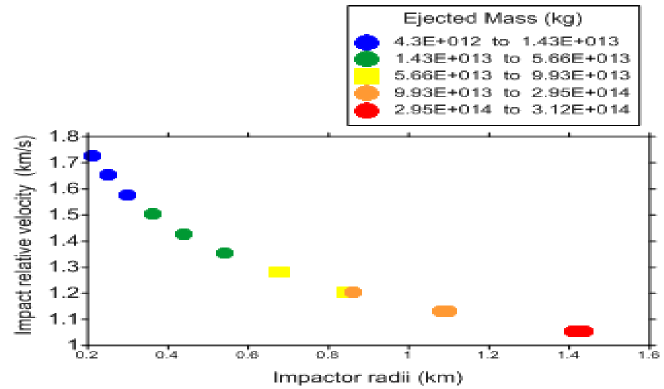
Ejected Mass (kg)
4.3E+012 to 1.43E+013
1.43E+013 to 5.66E+013
5.66E+013 to 9.93E+013
9.93E+013 to 2.95E+014
2.95E+014 to 3.12E+014
Impact relative velocity (km/s)
Impactor radii (km)

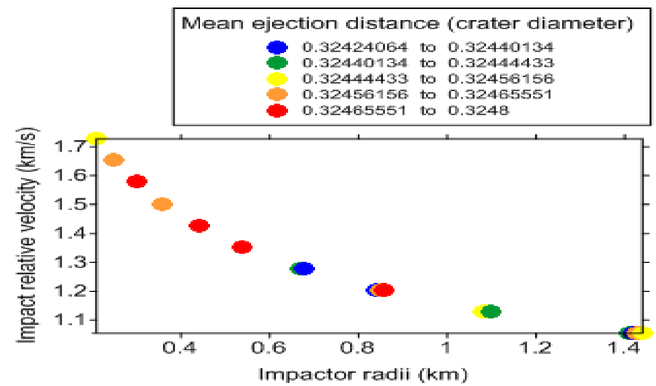
Mean ejection distance (crater diameter)
0.32424064 to 0.32440134
0.32440134 to 0.32444433
0.32444433 to 0.32456156
0.32456156 to 0.32465551
0.32465551 to 0.3248
Impact relative velocity (km/s)
Impactor radii (km)

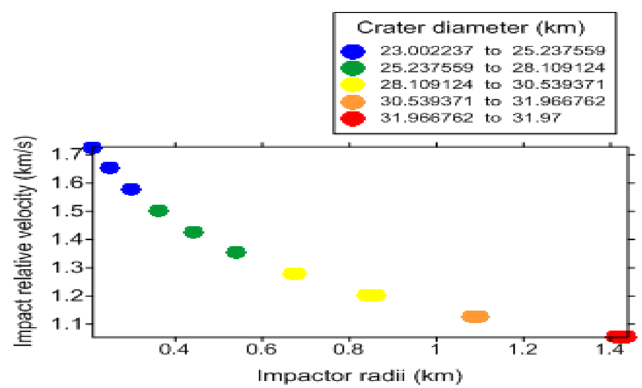
Crater diameter (km)
23.002237 to 25.237559
25.237559 to 28.109124
28.109124 to 30.539371
30.539371 to 31.966762
31.966762 to 31.97
Impact relative velocity (km/s)
Impactor radii (km)

Summary of results

- Mass ejected in the ring location: $4.3\ 10^{12} kg \rightarrow 3.2\ 10^{13} kg$ (*)
- Total mass displaced: $4.3\ 10^{12} kg \rightarrow 8.4\ 10^{17} kg$
- Impactor Radii: $0.2\ \rightarrow 1.6 km$
- Impact Velocities: $1.0\ \rightarrow 1.8 kms^{-1}$
- Diameter of craters: $23.0\ \rightarrow 32 km.$

Timescales for the event

At the present location of (10199) Chariklo

Impacts on Uranus or Neptune: (Levison et al. 2000)
$n_{U\&N} = 3.410^{-4} yr^{-1}$,

Scaling to the cross section of the asteroid:

$$\boxed{n_{CH} \sim 2.210^{-8} yr^{-1}.}$$

In the trans-Neptunian belt:

$$\boxed{n_{CHTN} \approx \pi A^2 P_I C (R_1^{-q} - R_2^{-q}) = 4 \times 10^{-12}\ yr^{-1}}$$ (Delloro et al. 2013)

Where:
Intrinsic probability of collisions: $P_I = 1.2910^{-22} km^{-2} yr^{-1}$
Mean relative velocity: $v_r(TN) = 1.65 kms^{-1}$
Size distribution: $C = 4.710^4$, $q = 4.2$
Size limits: $R_1 = 0.2km$, $R_2 = 1.6km$

Catastrophic collision on a satellite

We assume:

$M_{Sat} \approx M_{Ring}$

Breakup law: (Benz and Asphaug 1999):

$$\boxed{\frac{M_{LR}}{M_{Sat}} = -s\left(\frac{K_i}{Q^*} - 1\right) + \frac{1}{2} \sim \frac{1}{2}}$$

where:

$Q^* \approx 210^{-6} erggr^{-1}$

$m_i = \frac{4}{3}\pi\gamma_i\rho_i A_i^3,$

Hence:

$$A_i = \left(\frac{3}{2\pi\rho_i\gamma_i}\frac{Q^* M_{Sat}}{v_i^2}\right)^{1/3}$$

And: $\boxed{A_i \approx 150m, \text{ where we assume, } v_i = 3kms^{-1}}$

Timescale at present location: $\boxed{n_{Sat} \approx 10^{-12} yr^{-1},}$

At the trans-Neptunian belt $\boxed{n_{Sat} \approx \pi A_{Sat}^2 P_I C A_i^{-q} = 5.5 \times 10^{-14} yr^{-1},}$

Discussion

- It is not clear that the rings lie inside the Classical Roche limit distance from the asteroid for a 1km-size satellite.
- A 5km-sized object would disrupt at the ring location, taking into account the strength of the material.
- Tidal evolution is to slow to produce the approximation of a 1-km satellite to its breakup distance about (10199) Chariklo. A 100-km "binary satellite" would approach its distruption distance in the dynamical time of the asteroid. A large fraction of mass must be loss in this scenario.
- If the presently observed roration period of ~ 7hs is confirmed -and primordial, the tidal approach is highly unlikely, given the rotation rates distribution observed in the Solar System. The co-rotation period at the present ring location is ~ 20hs.
- Both collision scenarios are physically plausible, but the estimated timescales are longer than the dynamical lifetime of a Centaur asteroid, assuming typical impact probabilities taken form the literature (see for example Levison et al. 2000).
- A suitable collision on the body of the asteroid becomes almost certain on the dynamical lifetime of the asteroid if collision rates as suggested by observations of impacts on the major planets are assumed (about 1 order of magnitude larger than the ones estimated with numerical simulations, Hueso et al. 2013).
- The collsional scenarios are size-dependent, but it remains to be explained why all the observed larger bodies do not posses rings.
- With slight modifications the same arguments can be made for the case of (2060) Chiron.